J Mater Sci (2009) 44:244–249
DOI 10.1007/s10853-008-3075-2

Compositional dependence of structural and electrical properties in $(1 - x)$[PMN–PT(65/35)]–xPZ solid solutions

Lin Wang · Qiang Li · Zhiguo Xia · Wenxun Yan

Received: 24 July 2008 / Accepted: 20 October 2008 / Published online: 27 November 2008

Abstract Perovskite types $(1 - x)$[PMN–PT(65/35)]–xPZ (with $x = 0$, 0.1, 0.3, 0.5, 0.7 and 0.9) piezoelectric ceramics were prepared by a modified columbite precursor method. The lattice parameters of the $(1 - x)$[PMN–PT(65/35)]–xPZ ceramics increase with the addition of larger Zr^{4+} ion compared to that of other B-site ions. The SEM photographs of all the samples with different PZ content exhibit homogeneous and dense microstructure. The *P–E* loops indicate the PMN–PT–PZ ternary system has excellent ferroelectric properties. Both d_{33} and k_p dependences in PZ content show similar variation. Introduction of a small amount of PZ content in the PMN–PT(65/35) ceramics enhanced the relaxor behavior, which was confirmed by studying frequency and temperature-dependent dielectric behavior. The increasing values of diffuseness parameter obtained from the fit of a modified Curie–Weiss law established the relaxor nature.

Introduction

Piezoelectric materials, represented by $Pb(Mg_{1/3}Nb_{2/3})O_3$-$PbTiO_3$ (PMN–PT), $Pb(Zn_{1/3}Nb_{2/3})O_3$-$PbTiO_3$ (PZN–PT), are crucial in medical ultrasonic imaging, telecommunication, and sonar systems [1–3]. For example, lead-based complex perovskite relaxor ferroelectrics PMN and the normal ferroelectric PT can form a solid solution, providing many compositions that have excellent electromechanical properties, which are useful in electrostrictive and piezoelectric transducer and actuator applications [4–6]. However, the high piezoelectric response has been associated with the morphotropic phase boundary (MPB), which is located in the range of $x = 0.30$–0.40 in $(1 - x)$PMN–xPT system as reported previously [7]. Recent studies have shown PMN–PT(65/35) to exhibit the highest piezoelectric properties for the $(1 - x)$PMN–xPT system. It is also accepted that the Curie temperature (*T*c) in this system is sensitive to the content of PT, furthermore, higher PT concentration will correspond to weak relaxation degree, and low rhombohedral to tetragonal phase transition temperature [8]. However, introduction of orthorhombic structure compound PZ into $(1 - x)$PMN–xPT system can stabilize the rhombohedral structure in this ternary system and increase the *T*c to some extent [9, 10]. Moreover, some recent studies also imply that the doping of $PbZrO_3$ (PZ) will result in the improvement of the diffuse phase transition behavior in some lead-based complex perovskite relaxor ferroelectrics ceramic systems [11, 12].

In our previous studies, we have primarily studied [13] that a small addition of PZ into the PMN–PT(65/35) system, the composition of which is near the MPB, increased the diffuse phase transition as well as the rhombohedral to tetragonal phase transition temperature $T_{R\text{-}T}$. In this article, we have systematically studied the phase formation and dielectric relaxor properties of $(1 - x)$[PMN–PT(65/35)]–xPZ, x = 0.1, 0.3, 0.5, 0.7, 0.9, ternary system. Considering that the B-site distribution is related to the relaxor behavior as well as other dielectric properties, a modified columbite precursor method was applied on the preparation of solid solution of $(1 - x)$[PMN–PT(65/35)]–xPZ. On this basis, this study also aims to provide further information on the dielectric and piezoelectric properties, especially the relaxor behaviors of the ternary ceramic systems.

L. Wang · Q. Li (✉) · Z. Xia · W. Yan
Department of Chemistry, Tsinghua University, Beijing 100084, People's Republic of China
e-mail: qiangli@mail.tsinghua.edu.cn

L. Wang
e-mail: wanglin00@mails.tsinghua.edu.cn

Experimental procedure

A series of compositions was selected according to the proposed compositions of $(1 - x)$[PMN–PT(65/35)]–xPZ with x = 0, 0.1, 0.3, 0.5, 0.7, and 0.9 (hereafter denoted as S1, S2, S3, S4, S5, and S6). Reagent-grade oxide powders of PbO, MgO, Nb_2O_5, TiO_2, and ZrO_2 were used as raw materials. The columbite precursor method as described by Swartz and Shrout [14] was employed in the synthesis of $(1 - x)$[PMN–PT(65/35)]–xPZ. Nb_2O_5 was mixed with 2 mol% excess MgO and calcined at 1,000 °C for 6 h to form the columbite precursor $MgNb_2O_6$. Then $MgNb_2O_6$, PbO, TiO_2, and ZrO_2 powders were commixed according to the given composition with an addition of 3 mol.% excess PbO to compensate for losses, and the mixtures were fired at 850 °C for 2 h to obtain the perovskite structure. The powders obtained were subjected to axial pressing at 100 MPa to form disk specimens of 10 mm in diameter and of the order of a few millimeters thick. The disk specimens were sintered at 1,200 °C for 2 h in a lead-rich atmosphere. The lead atmosphere was provided by $PbZrO_3$ + 8 mol%ZrO_2 powders.

The phase formations of the sintered specimens were recorded by using X-ray powder diffractometer (D8 ADVANCE, Brüker, Germany, Cu Kα radiation, 40 kV, 40 mA). The density was determined by the Archimedes method in water to verify the qualities of these sintered samples, and the microstructure analyses were undertaken by a scanning electron microscopy (SEM: JEOL Model JSM 840A). Grain size was determined from SEM micrographs by a linear intercept method. Then the sintered samples were polished and covered with silver paste as the electrode for the dielectric measurement. Dielectric properties of the sintered ceramics were studied as functions of both temperature and frequency using an HP4192A Precision LCR meter connected to a computer automatic measurement. The piezoelectric constant d_{33} was measured using a quasistatic piezo-d_{33} meter (Institute of Acoustics, Chinese Academy of sciences, ZJ-2) after the samples were poled under 30 kV/cm dc field at 120 °C for 15 min in silicon oil and aged for 24 h.

Results and discussions

Compositional dependence of structural properties for $(1 - x)$[PMN–PT(65/35)]–xPZ ceramics

The X-ray diffraction (XRD) patterns of S1–S6 are shown in Fig. 1. The results reveal that all the samples are of the pure perovskite structure. It is known that in the rhombohedral phase, the {200} profile will show a single narrow peak because all the planes of {200} share the same lattice

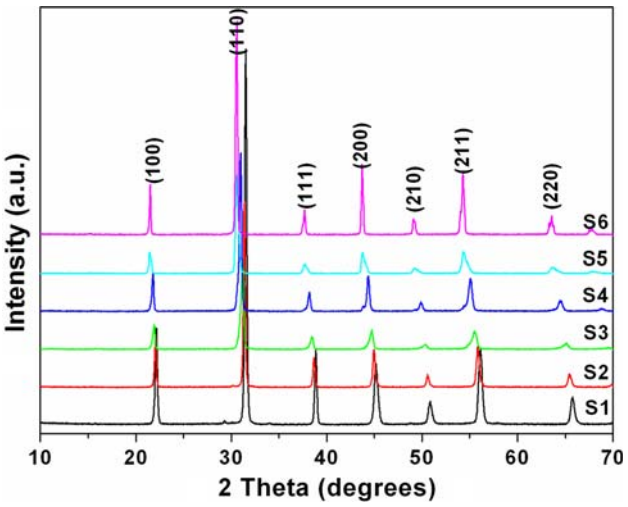

Fig. 1 XRD patterns of $(1 - x)$[PMN–PT(65/35)]–xPZ ceramics for various compositions

parameters, while in the tetragonal phase, the {200} profile should split into two peaks with the intensity height of one being half of the other because the lattice parameters of {200} and {020} are the same but are slightly different from those of {002}. Around $2\theta = 45$ °C as shown in Fig. 1, single {200} peak of all the samples demonstrates that the phase structure of them is rhombohedral phase. Introduction of rhombohedral structure compound PZ into $(1 - x)$PMN–xPT system indeed stabilizes the rhombohedral structure in this ternary system. From the XRD patterns, with the increase of PZ content, the peaks are moving to lower degree gradually. Compared to other B-site ions, Zr^{4+} ion has the largest ion-radius. With the addition of larger Zr^{4+} ion, the lattice parameters of these samples are increased; Performance on the patterns, allows the peaks move to lower degree. And, according to the XRD patterns, we can calculate the lattice parameters of

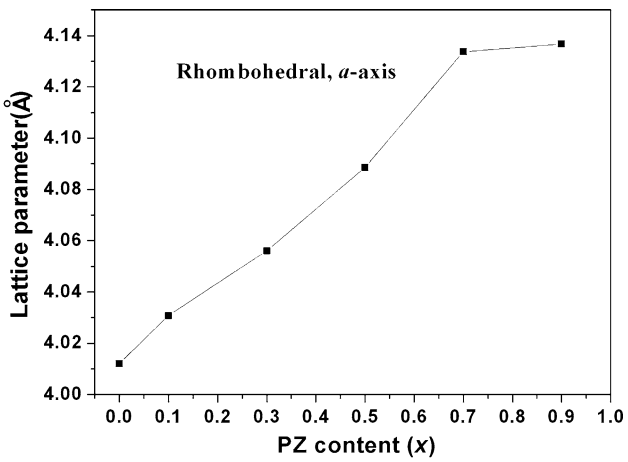

Fig. 2 PZ content dependence of lattice parameter for $(1 - x)$[PMN–PT(65/35)]–xPZ ceramics

$(1 - x)$[PMN–PT(65/35)]–xPZ ceramics as shown in Fig. 2. It confirmed the a-axis is gradually increasing with the addition of PZ content.

To examine the microstructure of the ceramics, the SEM photographs of the fractured surfaces from the samples with variable compositions sintered at 1,200 °C are shown in Fig. 3. It is seen that their microstructures are homogeneous without the second phase, as also verified by the XRD analysis. In addition, for all the compositions, the fracture characteristics are intergranular fracture with some transgranular fracture, indicating dense microstructure obtained [15] and the formation of the complete solid solution without any second phase. There is a grain growth trend with the increase of PZ content. S1 sample shows the smallest grain size ($\sim$2 μm), and the grain grows to about 5 μm in S6 sample.

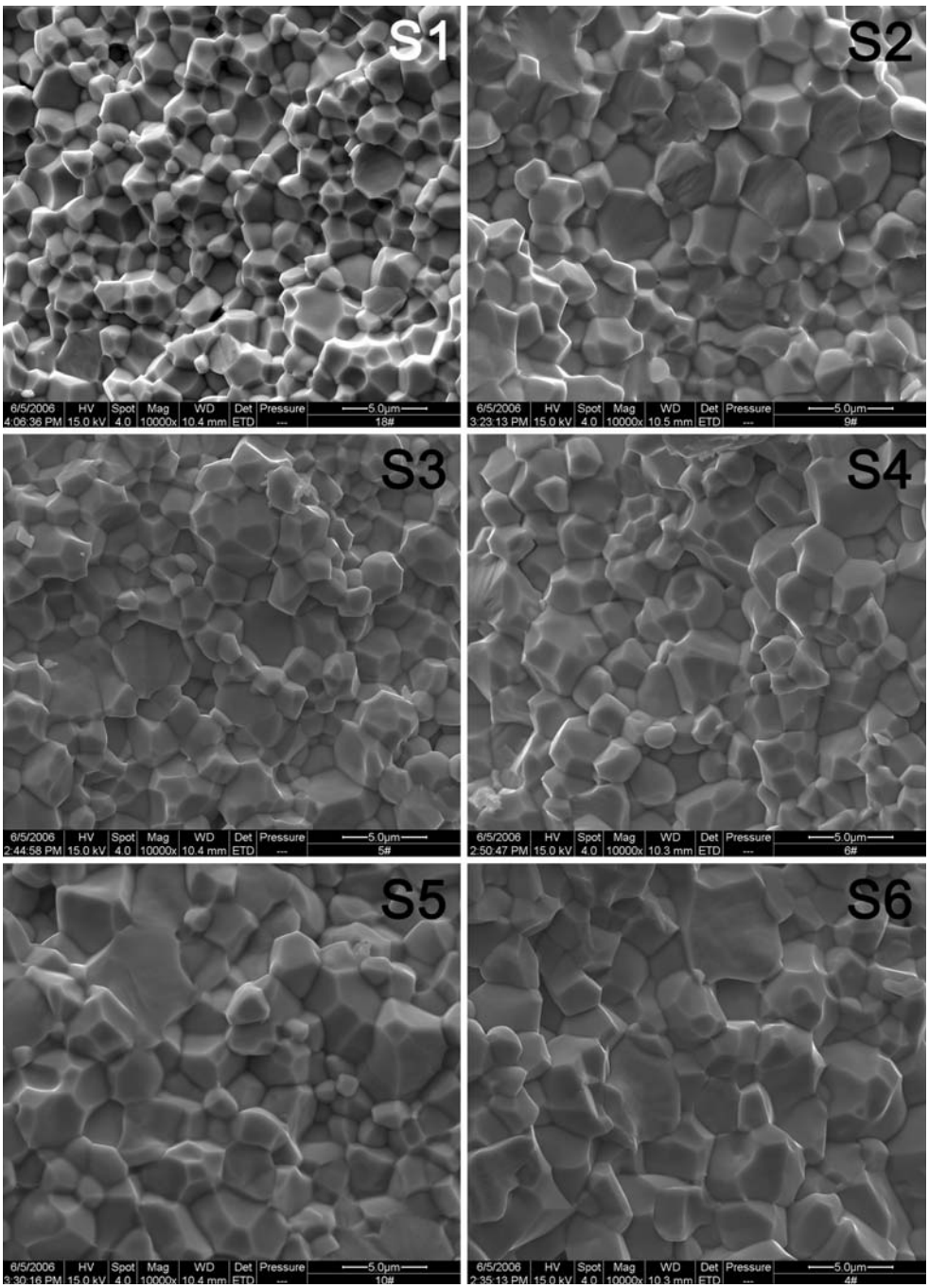

Fig. 3 SEM images of the $(1 - x)$[PMN–PT(65/35)]–xPZ ceramics sintered at 1,200 °C for 2 h

Room temperature electrical properties

The room temperature *P–E* hysteresis loops of $(1 - x)$[PMN–PT(65/35)]–*x*PZ ceramics are illustrated in Fig. 4. They all exhibit well-saturated *P–E* loops, which means the PMN–PT–PZ ternary system has excellent ferroelectric properties. The values of remnant polarization (P_r) and coercive field (E_c) can be evaluated from the respective saturated ferroelectric hysteresis loop in Fig. 4. Furthermore, the compositional dependences of P_r and E_c for $(1 - x)$[PMN–PT(65/35)]-*x*PT ceramics at room temperature are given in Fig. 5. The value of P_r decreases and then increases with increasing PZ content and that the value of E_c increases steadily with the PZ content increasing. The maximum values of P_r and E_c are both observed in the 0.9 PZ content compositions, namely, that of 38.6 μC/cm^2 and 11.79 kV/cm, respectively. Because of the coexistence of

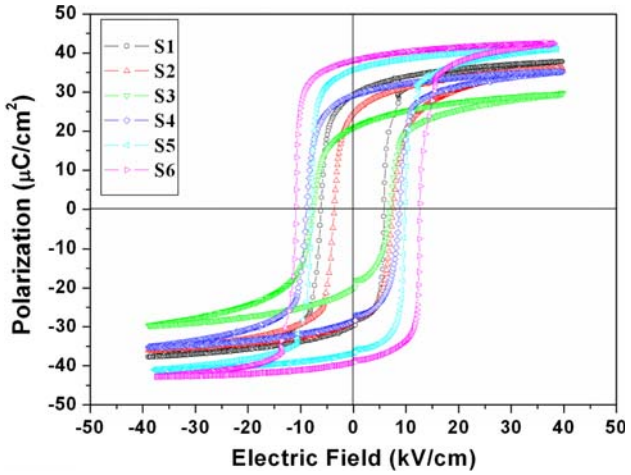

Fig. 4 Polarization *P–E* hysteresis curves of the $(1 - x)$[PMN–PT(65/35)]–*x*PT ceramics

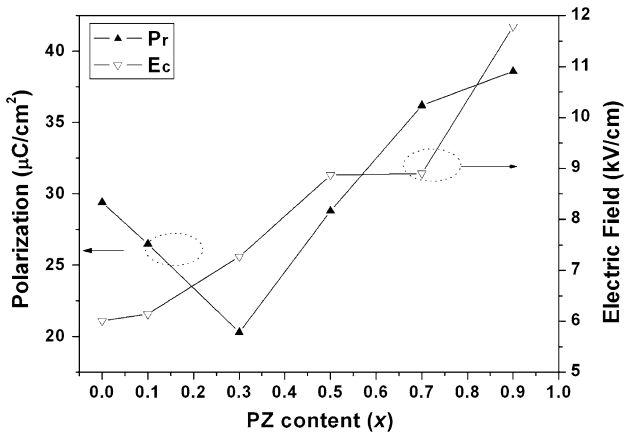

Fig. 5 Compositional dependence of remnant polarization P_r and coercive field E_c for $(1 - x)$[PMN–PT(65/35)]–*x*PT ceramics at room temperature

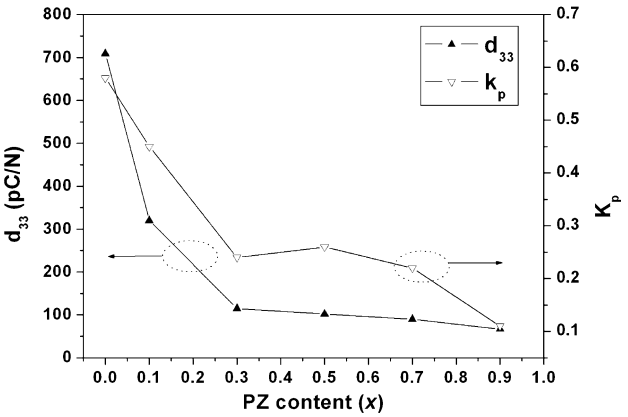

Fig. 6 Compositional dependence of piezoelectric coefficient d_{33} and electromechanical coupling coefficient k_p for $(1 - x)$[PMN–PT(65/35)]–*x*PT ceramics at room temperature

rhombohedral and tetragonal phase, the compositions near the MPB have 14 possible polarization directions [16]. The large numbers of the polarization direction cause enhanced crystallographic orientations under the electric field and, in turn, result in high polarization, dielectric, and piezoelectric properties. However, the rhombohedral phase has more reorientational direction than the tetragonal phase, which therefore, could achieve a larger remnant polarization [17]. Consequently, with the addition of PZ content, the composition of samples transforms from MPB to rhombohedral phase, and the value of P_r decreases and then increases.

The variations of the piezoelectric coefficient d_{33} and electromechanical coupling coefficient k_p for $(1 - x)$[PMN–PT(65/35)]–*x*PZ ceramics with compositions $x = 0$, 0.1, 0.3, 0.5, 0.7, and 0.9, are given in Fig. 6. As we can see, both d_{33} and k_{33} dependences in PZ content shows similar variation. The primary PMN–PT(65/35) ceramic has the best piezoelectric properties, the maximum value of d_{33} is 705 pC/N and that of k_p is 0.59 pC/N. From the structural analysis, it follows that the compositions with the best piezoelectric properties correspond to the composition near the MPB, which is consistent with the previous report on PMN–PT–PZ system [12, 17]. With small addition of PZ content, the phase of samples moves from MPB to rhombohedral structure, and the values of d_{33} and k_p decrease sharply from $x = 0$ to 0.3. With further addition of PZ, the phase of samples is far away from MPB, and the values decrease slightly from $x = 0.3$ to 0.9. For practical application of the ternary system $(1 - x)$[PMN–PT(65/35)]–*x*PZ, it is worthwhile for further research in the range of $0 < x < 0.3$.

Relaxor behavior of $(1 - x)$[PMN–PT(65/35)]–*x*PZ ceramics as a function of composition

The temperature dependences of dielectric constant for S1–S6 samples with different frequencies (1, 10, and 100 kHz)

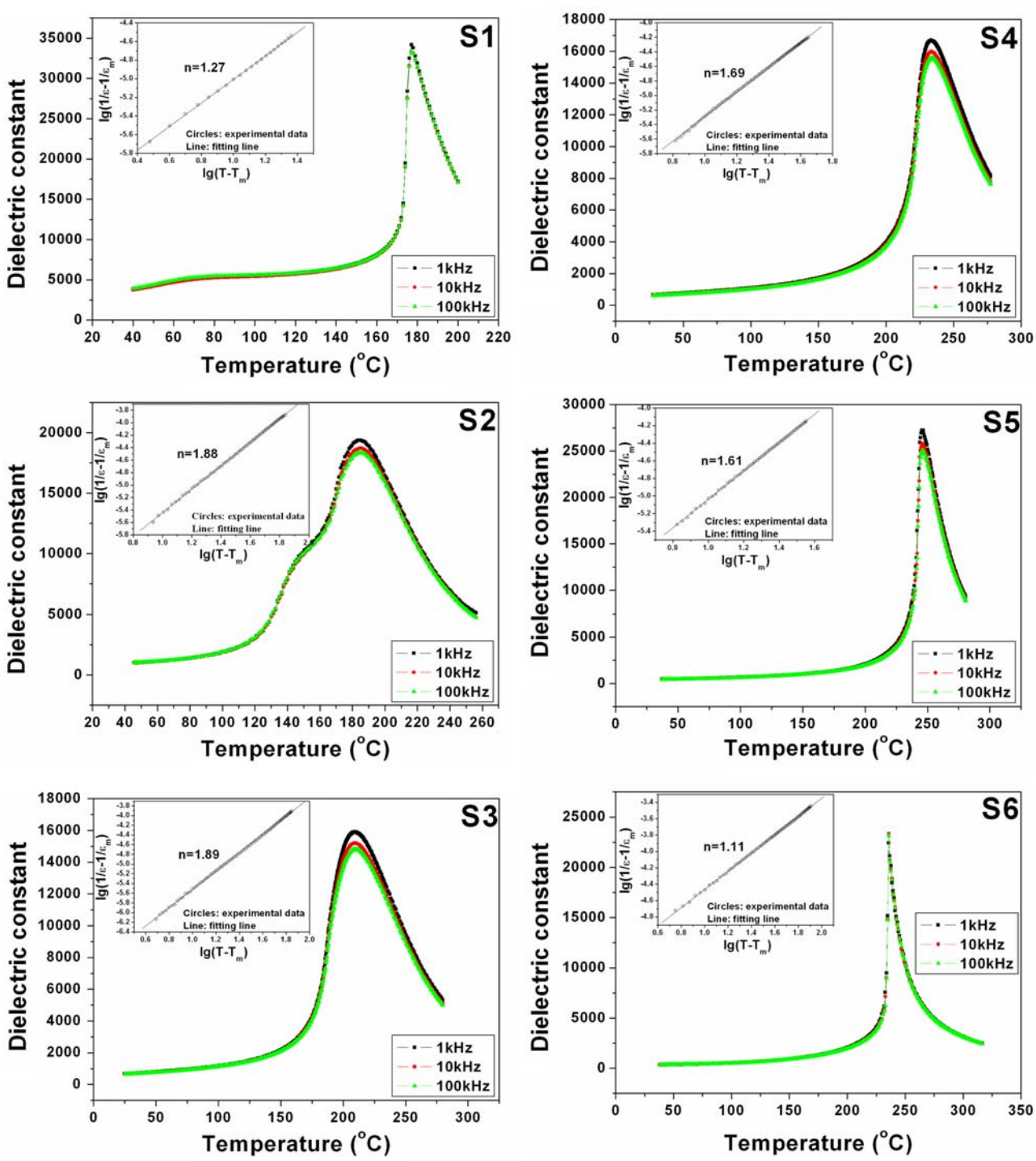

Fig. 7 Temperature dependence of dielectric constant at 1 kHz, 10 kHz, and 100 kHz for $(1 - x)$[PMN–PT(65/35)]–xPT ceramics. The insets show the dependence of $\lg(1/\varepsilon - 1/\varepsilon_m)$ with $\lg(T - T_m)$ at 1 kHz

are illustrated in Fig. 7. Obviously, as shown in S1 sample, the primary PMN–PT(65/35) ceramics with the composition located in the MPB region exhibit more of normal ferroelectric behavior. And the dielectric peak around *Tc* is sharp, which corresponds to the low extent of diffuse phase transition. With the small introduction of PZ content ($x = 0.1$), the dielectric peak broadens rapidly, which means the relaxor behavior of the ceramics has been enhanced. The enhanced diffuse phase transition in $Pb(B'_{1/3},B''_{2/3})O_3$-type perovskites suggests that more 1:1 short-range ordered micro-domains have formed [10]. Because the average Mg:Nb ratio in the present PMN–PT–PZ system is 1:2, the

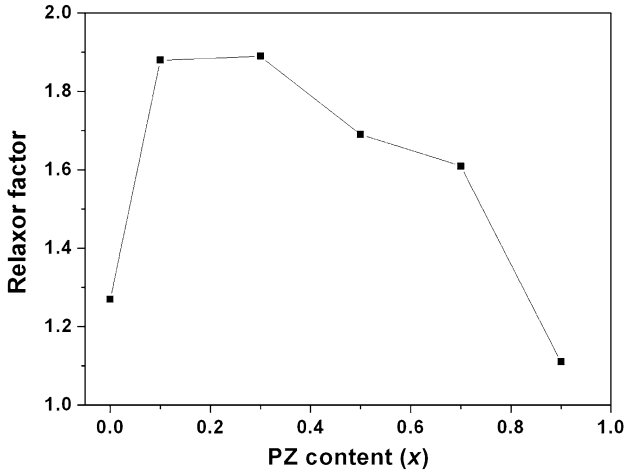

Fig. 8 PZ content (x) dependence of the relaxor factor α

enhanced 1:1 short-range ordering of Mg:Nb in the presence of PZ thus expedites the B-site compositional fluctuation occurring on a nanometer scale [9]. However, with more addition of PZ, the content of relaxor PMN is decreased; then the enhancement mentioned before is not the dominant effect to the relaxor behavior of samples. The dielectric peak becomes sharper with less content of PMN [18]. When $x = 0.9$, the curve of 0.1[PMN–PT(65/35)]-0.9PT sample is close to the normal ferroelectrics.

In General, the structure transformations of ferroelectric ceramics can be reflected from the shape of dielectric peak. In order to estimate the diffuse phase transition of relaxor ferroelectrics quantitatively, their dielectric characteristics are known to deviate from the typical Curie–Weiss behavior and can be described by a modified Curie–Weiss relationship [19]:

$$\frac{1}{\varepsilon} - \frac{1}{\varepsilon_m} = \frac{(T - T_m)^{\alpha}}{C} \quad (1)$$

where α and C are both material constants depending on the composition of the samples. The parameter α gives information on the character of the phase transition: for $\alpha = 1$, a normal Curie–Weiss law is obtained; $\alpha = 2$ describes a complete diffuse phase transition. The inset of Fig. 7 in every sample shows the plot of $\lg(1/\varepsilon - 1/\varepsilon_m)$ as a function of $\lg(T - T_m)$ at 1 kHz. According to Eq. 1, the value of α can be calculated from the slopes of inset after linear fitting and the variation of relaxor factor α with increasing PZ content (x) is shown in Fig. 8. The trend of the curve is corresponding with the results discussed above.

Conclusion

Perovskite types $(1 - x)$[PMN–PT(65/35)]–xPZ (with $x = 0$, 0.1, 0.3, 0.5, 0.7, and 0.9) piezoelectric ceramics were prepared by a modified columbite precursor method. With the addition of larger Zr^{4+} ion compared to that of other B-site ions, the lattice parameters of the $(1 - x)$ [PMN–PT(65/35)]–xPZ ceramics are increased. As a result the peaks move to lower degree on XRD patterns. The SEM photographs of all the samples with different PZ content exhibit homogeneous and dense microstructure. The P–E loops indicate the PMN–PT–PZ ternary system has excellent ferroelectric properties and the maximum values of P_r and E_c are both observed in the 0.9 PZ content compositions, namely, that of 38.6 μC/cm^2 and 11.79 kV/cm, respectively. Both d_{33} and k_p dependence in PZ content shows similar variation and the values of them decrease sharply from $x = 0$ to 0.3. The frequency and temperature dependences of dielectric constant show the relaxor behavior of PMN–PT(65/35) ceramics has been enhanced with small amount of PZ content but decreased by further addition of PZ content. The values of diffuseness parameter obtained from the fit of a modified Curie–Weiss law established the relaxor nature.

References

1. Service RE (1997) Science 275:1878
2. Park S-E, Shrout TR (1997) J Appl Phys 82:1804
3. Park S-E, Shrout TR (1997) Mater Res Innov 1:20
4. Nomura S, Uchino K (1983) Ferroelectrics 50:197
5. Masuzawa H, Ito Y, Nakaya C, Takeuchi H, Jyomura S (1989) Jpn J Appl Phys 28:101
6. Yamashita Y, Hosono Y, Harada K, Yasuda N (2002) IEEE Trans Ultrason Ferroelectr Freq Control 49:184
7. Ari-gur P, Benguigui L (1975) J Phys D Appl Phys 8:1856
8. Hu XB, Wang JY, Ma LL, Xu XG, Luo HS, Zhu PP, Tian YL, Cryst J (2005) Growth 275:e1703
9. Harmer MP, Chen J, Peng P, Chan HM, Smyth DM (1989) Ferroelectrics 97:263
10. Chen J, Chan HM, Harmer MH (1989) J Am Ceram Soc 72:593
11. Jiang XP, Fang JW, Zeng HR, Chu BJ, Li GR, Chen DR, Yin QR (2000) Mater Lett 44:219
12. Xia ZG, Li Q (2007) J Phys D Appl Phys 40:7826
13. Xia ZG, Wang L, Yan WX, Li Q, Zhang L (2007) Mater Res Bull 42:1715
14. Swartz SL, Shrout TR (1982) Mater Res Bull 17:1245
15. Wang L, Li Q, Xue LH, Zhang YL (2007) J Phys Chem Solids 68:2008
16. Randall CA, Kim N, Kucera J, Cao W, Shrout TR (1998) J Am Ceram Soc 81:677
17. Yoon KH, Lee HR (2001) J Appl Phys 89:3915
18. Yimniruna R, Ananta S, Laoratanakul P (2005) J Eur Ceram 25:3235
19. Uchino K, Nomura S (1982) Ferroelectr Lett 44:55